A R C H I V E S O F M E T A L L U R G Y A N D M A T E R I A L S
Volume 51 2006 Issue 1

S. DYMEK*, M. WRÓBEL*, M. BLICHARSKI*

PROCESSING AND MICROSTRUCTURE OF A Ti-25Nb-22Al ALLOY

WYTWARZANIE I MIKROSTRUKTURA STOPU Ti-25Nb-22Al

The paper shows preliminary results of the processing and characterization of a Ti-25Nb-22Al (at.%) alloy. The alloy was synthesized by mechanical alloying followed by hot pressing at 1300°C. In the microstructure of the alloy two phases prevailed: Ti_3Al-based phase and Nb_3Al-based one. Minor amounts of titanium solid solution and oxide dispersoid were also found. Oxide dispersoid was introduced to the microstructure in order to improve strength and creep resistance at elevated temperatures. Preliminary mechanical tests showed that fracture toughness of the synthesized material, about 15 $MPa \cdot m^{0.5}$, is relatively high comparing to other intermetallis

Keywords: intermetallics, mechanical alloying

Praca obejmuje wyniki wstępnych badań nad wytwarzaniem i własnościami stopu Ti-25Nb-22Al (at.%). Stop wytworzono metodą mechanicznej syntezy połączoną z późniejszą konsolidacją proszków przez prasowanie pod ciśnieniem w temperaturze 1300°C. W mikrostrukturze wytworzonego stopu przeważały dwie fazy: jedna na osnowie fazy międzymetalicznej Ti_3Al, a druga na osnowie Nb_3Al. Obok tych faz występował jeszcze roztwór stały na osnowie Ti oraz dyspersoid tlenkowy. Dyspersoid tlenkowy został wprowadzony do mikrostruktury w celu poprawy wytrzymałości i odporności na pełzanie w podwyższonej temperaturze. Wstępne badania mechaniczne wykazały, że odporność na pękanie wytworzonego stopu, około 15 $MPa \cdot m^{0.5}$, jest stosunkowo duża w porównaniu do innych stopów na osnowie faz międzymetalicznych.

1. Introduction

The aerospace and automotive industry is looking forward to the development of new materials that are stronger, lighter and have a higher temperature potential compared with presently available alloys. Intermetallics based on the α_2-Ti_3Al compound have been long ago recognized as potential materials for the mentioned applications. However, the binary alloys do not possess acceptable balance of mechanical and other essential properties. It was shown that addition of niobium can improve room temperature ductility of these alloys [1]. An intensification of research on the Ti-Al-Nb system started in the late 1980s when Banerjee et al. [2] discovered a ternary intermetallic compound based on the stoichiometry Ti_2AlNb with orthorombic crystal structure which was designated as the O phase. Since then the new alloy family, so called "orthorombic alloys", has received considerable attention [3-6]. All that studies confirmed strong sensitivity of mechanical properties to the microstructure, especially phase content of the Ti_2AlNb-based alloys. Since the microstructure depends on a processing route and further thermomechanical treatment, therefore, optimization of these two factors is the key issue in potential application of these alloys.

Mechanical alloying turned out to be a viable technique especially for producing creep resistant materials [7]. Also, as a solid state process, it is particularly useful in synthesis of metals with large difference in melting points like Nb and Al [8]. This paper shows preliminary results concerning processing and microstructural characterization of a Ti-25Nb-22Al (at.%) alloy. In particular, characterization by transmission and scanning electron microscopy of both powder and the compacted material was carried out during this stage of research.

2. Materials and experimental procedure

The alloy with the target chemical composition of Ti-25Nb-22Al (at.%) was synthesized by mechanical alloying in a Szegvari-type attritor. The starting pow-

* AGH UNIVERSITY OF SCIENCE AND TECHNOLOGY, FACULTY OF METALS ENGINEERING AND INDUSTRIAL COMPUTER SCIENCE, 30-059 KRAKÓW, AL. MICKIEWICZA 30, POLAND

der mixture consisted of elemental Ti (99% pure), Nb (99.8% pure) and Al (99.5% pure) with particle size less than 44 μm (-325 mesh). Mechanical alloying was carried out in an argon atmosphere with the controlled oxygen level reduced to less than 10 ppm. This was accomplished by using a positive pressure of 20 kPa in the milling chamber. The milling was carried out in a sealed stainless steel tank with a 3.63 kg (8 lb) charge of 4.76 mm (3/16") stainless steel balls and a 12:1 ball to powder ratio (by weight). In order to prevent agglomeration of the relatively ductile powders on the shaft and milling chamber walls, the initial four hours of milling was carried out at cryogenic temperature, using liquid nitrogen as the coolant. During the milling, powder samples were taken out after 10, 20, 50 and 100 hours (the total milling time), allowing for characterization of the powder morphology and the progress of mechanical alloying process. The powders collected at the end of milling, i.e. after 100 h of milling, were sieved through a 44 μm mesh and consolidated by hot pressing in the argon atmosphere at pressure 25 MPa and temperature 1300°C.

The changes in particle morphology and chemical composition during milling were examined by a scanning electron microscope. The phase analysis was performed with CoKα radiation. The X-ray spectra were used for evaluation of lattice parameters, lattice strains and X-ray crystallite size. Microstructure of the compacted material was characterized by scanning electron microscopy (SEM) with utilization of the Z contrast produced by backscattered electrons (BSE) and also by transmission electron microscopy (TEM) supplemented by the energy dispersive spectrometry (EDS). The measurement of chemical compositions of constituent phases, both in SEM and TEM, was performed by a standardless method which total all elements to 100%. Light elements analysis was not performed. Preliminary mechanical testing was limited to Vickers hardness measurements and determination of K_{Ic} from microcraks propagating from indent corners.

3. Results and discussion

Powder

The initial powder blend was composed of relatively large, ca 40 μm, titanium and niobium particles and evenly dispersed smaller, ca 5-10 μm, aluminum particles (Fig. 1). Different particles were distinguished by the point EDS analysis as well as EDS mapping. Evolution of particle size and morphology during the course of milling was typical for milling of ductile powders [9, 10]. Initially, the increase in particle size from the initial starting blend was observed. This was due to the predominance of welding over fracturing occurring in the relatively soft particles. Most particles were round and flat. Many of them approached size about 500 μm.

Fig. 1. SEM image of initial powder blend

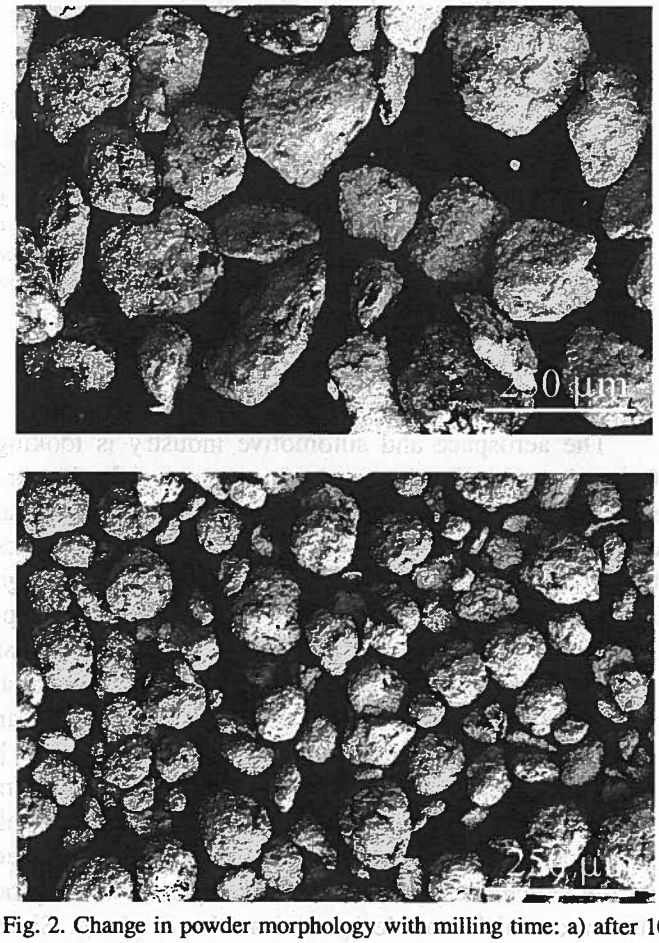

Fig. 2. Change in powder morphology with milling time: a) after 10 h, b) after 100 h

However, there was a significant scatter in particle size. With milling time the shape of particles changed to more spheroidal. After 50 hours of milling particles become much finer indicating predominance of fracturing but the rough particle surface showed that welding was still in

work. The 100 hours of milling produced uniform powder with almost spherical particles with smooth surfaces. Fig. 2 shows the difference in powder particle morphology after 10 and 100 hours of milling. The average size of powder particle (after sieving through a 45 μm mesh) was about 10 μm. EDS point and map analysis showed that the chemical composition of individual particles was uniform and corresponded to the starting composition of powder blend.

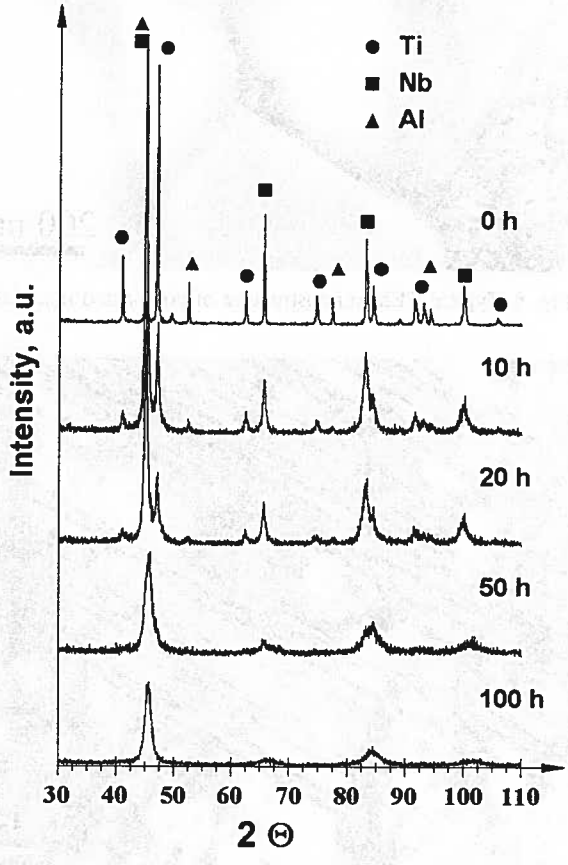

Fig. 3. The composed figure of X-ray diffractograms after 0, 10, 20, 50 and 100 h of milling

The diffractograms obtained from powders after 0, 10, 20, 50, and 100 h of milling are shown in Fig. 3. In general, with the milling time peaks became broader and their intensities decreased. The peak broadening was due to refinement of powder and due to strains associated with intense plastic deformation of powder particles during milling. It is interesting that positions of peaks did not change with milling time indicating no change in lattice parameters of the alloy with milling time. It is not typical behavior but may result from very small difference in atomic radii of constituent elements (Ti – 146 pm, Nb – 143 pm, Al – 143 pm). The peak positions as well as the change in crystallite size and lattice strain with milling time for Nb is shown in Table 1.

TABLE 1
The change in crystallite size and lattice strain for Nb peaks

Milling time, h	Peak position, deg	Crystallite size, nm	Lattice strain, %
0	66.300	245	0.068
10	66.300	30	0.424
20	66.300	18	0.459
50	66.300	4	2.024
100	66.300	3	2.393

Peaks from Al, though much weaker than in the starting powder (0 h), were still present till 20 h of milling and disappeared after 50 h indicating dissolution of Al in Nb or Ti. The fast dissolution of Al during milling was expected because Al is much faster diffuser both in Ti and Nb compared to Ti or Nb in Al, e.g. at room temperature, the diffusivity of Al in Ti is $1.06 \cdot 10^{-21}$ $cm^2 \cdot s^{-1}$ and that of Ti in Al is $2.9 \cdot 10^{-23}$ $cm^2 \cdot s^{-1}$ [10]. Peaks from Ti, on the other hand, become weaker and weaker with the milling time but were still present after 80 h of milling. After 100 h of milling only peaks from Nb solid solution were detected on X-ray diffractograms. The lack of peaks from Ti is a little puzzling since titanium constitutes the major component of the alloy (over 50 at.%). However, it was shown that prolonged milling of Ti and Al powders, regardless of the type of mill used, leads to the amorphisation of these powders [10]. On the other hand, Nb powders turn into an amorphous phase more difficult [11].

Compacted material

The microstructure of the compacted material revealed on images formed by backscattered electrons in a scanning electron microscope is shown in Fig. 4. Utilization of Z-contrast allowed for revealing phases

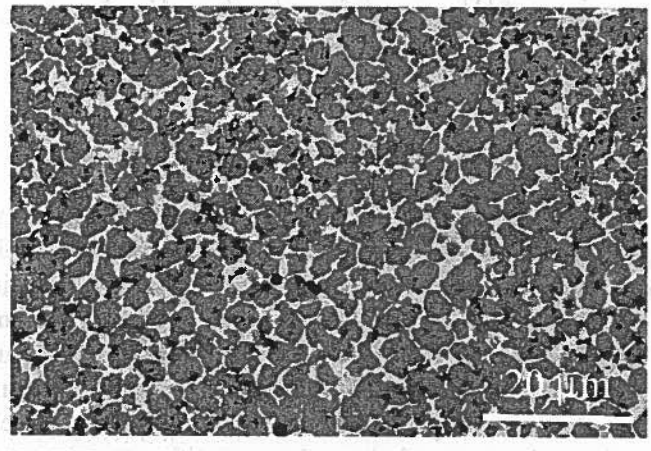

Fig. 4. Microstructure of compacted alloy, SEM BSE Z-contrast

with different concentration of constituent elements. Since backscattered electron yield is higher for higher Z (atomic number) the grains containing more Nb appear brighter. The darker phase corresponds to a phase with a lower content of heavier elements. Chemical compositions of bright and dark phases determined by EDS are given in Table 2. Small black particles in Fig. 4 are titanium and aluminum oxides.

TABLE 2

Chemical composition of constituent phases, at. %

Phase	Ti	Nb	Al
bright	47-50	34-36	15-17
dark	58-62	13-15	25-27

X-ray phase analysis revealed two phases based on hexagonal Ti_3Al ($D0_{19}$) and cubic Nb_3Al (A15) (Fig. 5). Titanium solid solution as well as minute amount of a hexagonal $Ti_{10}Al_3Nb$ was also detected. Neither the targeted orthorombic Ti_2NbAl phase nor, usually met in similar alloys, a phase with the B2 crystal structure were detected [4]. The lack of the B2 phase is detrimental to the alloy since the presence of this phase is essential in realizing room temperature ductility in these alloys. The likely reason for the absence of Ti_2NbAl and B2 phases is the relatively high temperature of powder compaction 1300°C, i.e. beyond O and B2 phase range [4].

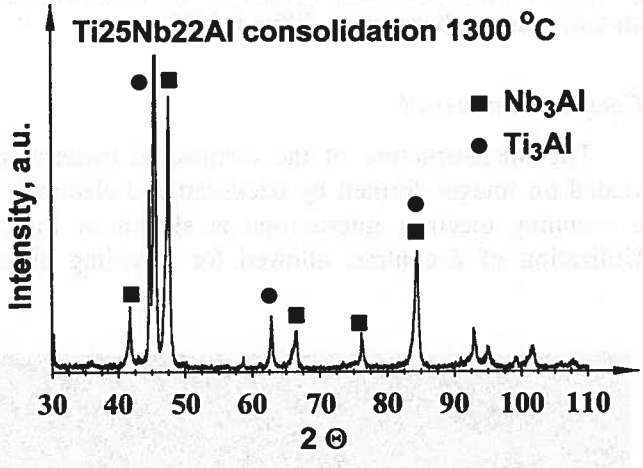

Fig. 5. X-ray diffractogram of consolidated material

TEM investigation confirm the presence and composition of the Ti_3Al- and Nb_3Al-based phases. Typical microstructure of consolidated material is shown in Fig. 6. Also the presence of Ti solid solution was confirmed. However, the Ti_3Al-based phase contained characteristic striations which differentiated this phase from the other ones (Fig. 7). Such contrast could be produced in the early stages of phase decomposition reaction and may in this case be evidence that the Ti_3Al-based phase began to transform to the orthorombic phase. Similar effect was observed in other studies [12]. This may indicate the need of further heat treatment applied to the as-compacted samples.

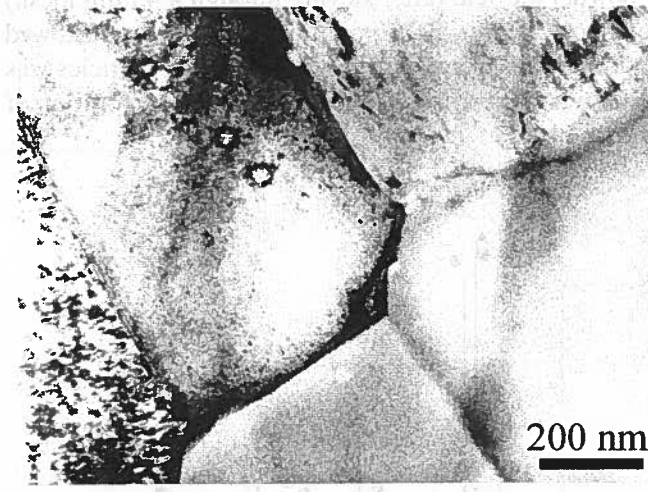

Fig. 6. Typical TEM microstructure of compacted material

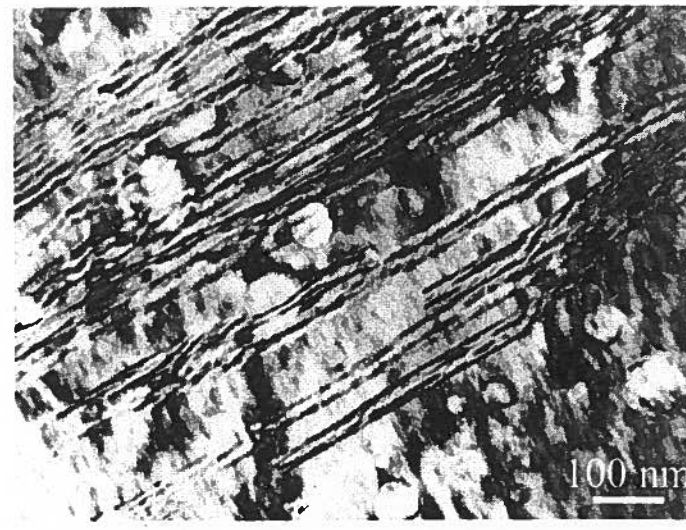

Fig. 7. Characteristic striations in the Ti_3Al-based phase

Room temperature Vickers hardness tests were performed in order to determine the fracture toughness K_{Ic} from cracks propagating at indentation corners. First microcraks appeared at the load of 98.1 N and were very short. The calculated K_{Ic} was about 15 MPa · $m^{0.5}$. The Vickers hardness was about 300 HV.

4. Conclusions

1. The mechanical alloying is a viable processing route for synthesis Ti_2NbAl-type alloys.
2. The produced alloy was mainly composed of Ti_3Al- and Nb_3Al-based phases with addition of dispersed titanium and aluminum oxides.

3. Preliminary mechanical tests showed that fracture toughness of the synthesized and examined material, about 15 MPa · $m^{0.5}$, is acceptable for this type of alloy.

Acknowledgements

The financial support from the Polish Ministry of Education and Science, grant no. 4 T08A 017 25, is greatly appreciated.

REFERENCES

[1] H. Winter, US patent no. 3 411 901 (1968).
[2] D. Banerjee, A. K. Gogia, T. K. Nandi, V. A. Joshi, Acta Metall. **36**, 871 (1988).
[3] L. A. Bendersky, W. J. Boettinger, F. S. Biancaniello, Mat. Sci. Eng. **A152**, 41 (1992).
[4] A. K. Gogia, T. K. Nandy, D. Banerjee, T. Carisey, J. L. Strudel, J. M. Franchet, Intermetallics **6**, 741 (1998).
[5] S. Li, Y. Cheng, X. Liang, J. Zhang, Materials Science Forum **795**, 475-479 (2005).
[6] L. Germann, D. Banerjee, J. Y. Guédou, J.-L. Strudel, Intermetallics **13**, 920 (2005).
[7] C. Suryanarayana, Progress in Materials Science **1**, 46 (2001).
[8] S. Dymek, A. Lorent, M. Wróbel, A. Dollar, Materials Characterization **375**, 47 (2001).
[9] J. S. Benjamin, Materials Science Forum **88-90**, 1 (1992).
[10] L. Lü, M. O. Lai, Mechanical Alloying. Kluwer Academic Publishers, (1998).
[11] D. Oleszak, M. Burzyńska-Szyszko, H. Matyja, J. Mater. Sci. Let. **3**, 12 (1993).
[12] D. E. Alman, C. P. Dogan, Met. Mat. Trans. **26A**, 2759 (1995).

Received: 5 January 2006.